JOURNAL OF SOLID STATE CHEMISTRY 95, 64–73 (1991)

Longitudinal–Transverse Splitting Effects in IR Absorption Spectra of MoO_3

KAZUO EDA

College of Liberal Arts, Kobe University, Tsurukabuto, Nada, Kobe 657, Japan

Received November 2, 1990; in revised form April 30, 1991

IR absorption spectra of MoO_3 powder were changed greatly by heat treatments which gave rise to changes in the size and morphology of crystallites, while the powder's Raman scattering spectra were not changed. The change in IR spectra was due to longitudinal–transverse splitting effects. The IR spectra were analyzed by a curve-resolution technique and the separating peaks were ascribed to vibrational modes based on unit cell group analysis by considering longitudinal–transverse splitting effects. © 1991 Academic Press, Inc.

Introduction

Assignments of vibrational modes of solids are very difficult. Vibrational spectra of MoO_3 have been studied by many of researchers, because MoO_3 shows sharp and intense Raman bands. Nevertheless, the assignments of its vibrational bands are not resolved completely and still remain a subject of discussion (*1–10*). The assignments so far proposed have been carried out by following three methods: (1) comparison with vibrational frequencies of other materials which have the corresponding vibrational modes on the basis of unit cell group analysis (*1–3*), (2) calculation of frequencies using a Valence Force Field (VFF) model based on unit cell group analysis (*6–8*), and (3) calculation of frequencies using either a VFF or a Urey-Bradley Field model based on molecular group symmetry (*9, 10*).

Py and Maschke (*8*) represented the vibrational frequencies of Raman active modes using an extension of the calculations of Beattie *et al.* (*6*), which falls under the category of method (2). The author recently reported that the changes in vibrational frequencies due to the transformation from MoO_3 to H_xMoO_3 could be explained by Beattie *et al.*'s method (*11*). These facts indicate that the assignments obtained by method (2) are suitable. However, precise assignments of IR active bands cannot be obtained even by method (2), because IR bands are influenced by longitudinal–transverse splitting effects. These effects cannot be dealt by unit cell group analysis (*12*).

In the present work, the author discusses the relation between the changes in IR and Raman spectra of powder MoO_3 with heat treatments, which change the size and/or morphology of crystallites. Secondarily, the author analyzes the IR spectra in detail by a curve-resolution technique, and then, considering longitudinal–transverse splitting effects, interprets them on the basis of the modes under the unit cell group analysis.

0022-4596/91 $3.00

Basic Background

Vibrations in Solids

Vibrations in solids are dealt with as waves ("vibration waves"). These are classified into two types of waves, transverse and longitudinal. The wave consisting of a vibration that takes place along paths at right angles to the propagation direction is "transverse," while that along the same direction is "longitudinal." IR active modes give rise to the dipole moment of the vibrational transition, μ. For the longitudinal wave, the dipole moment results in a "source" of an electric field, while for the transverse wave, it does not (*12*). This difference makes the frequency of a longitudinal wave (ν_{LO}) larger than that of a transverse wave (ν_{TO}), even though both waves are based on the same vibrational mode ("longitudinal–transverse splitting effects"). The frequencies are related as (*12*)

$$\nu_{LO}^2 = \nu_{TO}^2 + \frac{1}{\varepsilon_\infty}\left|\frac{\mathbf{E}_l}{\mathbf{E}}\right|\frac{A}{\pi}\left(\frac{\partial\mu}{\partial Q}\right)^2,$$

where ε_∞ is the high-frequency dielectric constant, $\mathbf{E}$, the electric field of incidence, $\mathbf{E}_l$, the local electric field around an oscillator, A, the number of ion pairs in a unit volume, and $\partial\mu/\partial Q$, the change in dipole moment generated by the vibration.

It is noted that a vibration with a large $|\partial\mu/\partial Q|$ shows a large difference in frequency between ν_{TO} and ν_{LO}. Then, such a vibration has a large integrated absorption intensity, because the intensity is proportional to $(\partial\mu/\partial Q)^2$.

Generally, the vibration waves propagate not only in directions perpendicular and parallel to the direction along which the vibration takes place, but also in general directions. For cubic crystals, waves propagating in a general direction resolve into transverse and longitudinal waves by splitting triply degenerate and mutually orthogonal modes. However, for crystals with lower symmetry, transverse and longitudinal waves are mixed. Thus, the properties of waves propagating in general directions are intermediate between those of transverse and longitudinal waves. The frequencies of such waves fall in the range between ν_{TO} and ν_{LO} depending on the relation between the directions of propagation and μ generated by the vibration (*12*); i.e., for such crystals even their bulk modes have a frequency between ν_{TO} and ν_{LO} depending on the directions of propagation. (MoO_3 belongs to the orthorhombic system and the space group is $P_{bnm} \equiv D_{2h}^{16}$.)

An IR absorption spectrum of a powder specimen is represented as a sum of absorption by numerous crystallites randomly orientated in incidence. Assuming that all crystallites have the same size and morphology, the sum is replaced by a sum of absorption for numerous incidence beams which propagate in a random direction in one crystallite. Because thickness of the crystallite for an incidence beam propagating along a crystallographic direction depends on the size and morphology, the absorption intensity and the extent of longitudinal–transverse splitting effects for the beam depend on the size and morphology. Thus, the IR bands are influenced in their peak frequencies and band widths by size and morphology. In powder specimens crystallites with different sizes and/or with different morphologies generally coexist. Such coexistence may allow appearance of more than two bands assigned to the same vibrational mode, because a difference in size and/or morphology indicates a different peak frequency and a different band width.

The Assignments Proposed Previously

The assignments so far proposed (*1–3, 5, 6, 9, 10*) for IR absorption bands of MoO_3 are summarized in Table I. The assignments made by various researchers disagree slightly, as do the observed band frequencies, and are not adequate. For IR active Mo–O stretching vibrations only two to four

TABLE I

ASSIGNMENTS OF INFRARED FREQUENCIES (cm^{-1}) IN PREVIOUS STUDIES

Method (1)		Method (2)	Method (3)	
Barraclough and co-workers (*1*, *2*)	Mattes and Schröder (*3*)	Beattie and co-workers (*5*, *6*)	Camelot *et al.* (*9*)	Ravikumar *et al.* (*10*)
		351 δMo–O2		350 ν_2 O–Mo–O sym. bend
371		371 δMo–O1	428 ν_4 deformation of the angle	373 ν_4 O–Mo–O asym. bend
487	485	505 νMo–O2		
590	570 νMo–O2	545 νMo–O2′	562 ν_2 deformation of the plane	
822	821 νMo–O3[a]		825 ν_3 antisymmetric valency vibration	
868	870 νMo–O2′	840 νMo–O3[a]	865 $\nu_{4\times2}$	850 ν_1 Mo–O sym. stretch
992 νMo–O1	996 νMo–O1	1004 νMo–O1	993 $\nu_4 + \nu_2$	1000 ν_3 Mo–O asym. stretch

[a] O3 and O3′ are equivalent under the discussion by unit cell group analysis.

modes are assigned, though seven modes are expected by unit cell group analysis.

ν_{TO} and ν_{LO} of Each Mode of MoO_3

The crystal structure of MoO_3 is known (*13*). Figure 1 shows its structural model. As shown in the figure, oxygen atoms in MoO_3 are divided into three types depending on the methods of connection with Mo atoms, where O2 and O2′, O3 and O3′ are equivalent, respectively. O1 is doubly bonded to a Mo atom. There are four vibrational modes concerning to the stretching vibrations of this bond according to unit cell group analysis. Two of them areRaman active. The others, which are shown in Fig. 2, are IR active. The B_{2u} mode gives rise to a large change in the dipole moment, while the B_{3u} mode gives rise to a small change. Based on this fact, it is possible to distinguish between these two modes. Distinctions among other IR active modes can be achieved by the same way. Fortunately, Py and Maschke calculated the vibrational frequencies of MoO_3 and evaluated the ν_{TO} and ν_{LO} of each IR active mode from IR reflection spectra of a MoO_3 single

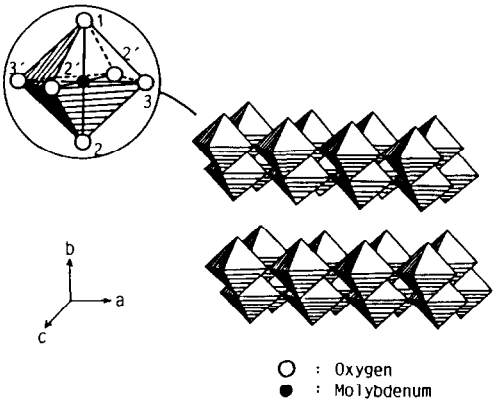

FIG. 1. A structural model of MoO_3.

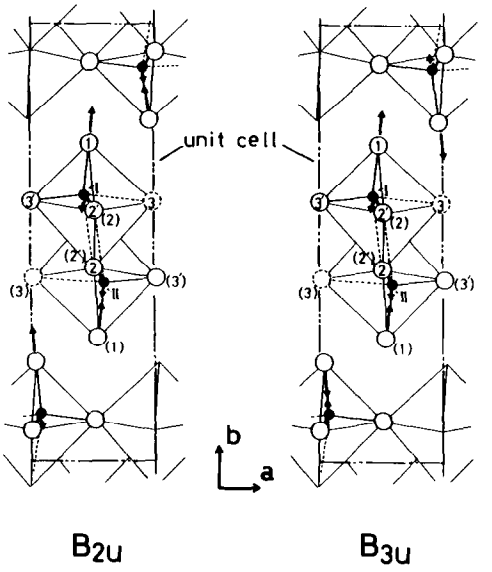

FIG. 2. IR active Mo–O1 stretching modes of MoO_3. The numbers in parentheses are given by the numbering for the Mo II atom.

crystal specimen (*7, 8*). These data, which are summarized in Table II, can be used as a guideline on assignments of IR bands of MoO_3.

Experimental

Heat Treatments and Measurements

Wako MoO_3 powder (grade 1) was used for experiments. The specimens were heated at suitable temperatures for suitable times in an air atmosphere, and were characterized by an X-ray diffraction (XRD) method, optical microscopy, and IR and Raman spectroscopy. XRD patterns were measured using a RIGAKU RINT 1200M diffractometer with Cu$K\alpha$ radiation. Optical micrographs were obtained using an ordinary optical microscope. IR absorption spectra were recorded on a Perkin–Elmer 1600 Fourier transform IR spectrometer and taken with 256 scans at 2 cm^{-1} resolution. For the measurement, the specimens were pressed into disks (ca. 0.5w% in KBr). Raman spectra were obtained using a JEOL JRS-400D Raman spectrophotometer with 514.5 nm excitation.

Curve Convolution

The IR spectra were analyzed by a curve-resolution technique, in which a convolution curve was fitted to an original curve by a least square method. Because the original curves were complicated, their second order and third order differential curves did not give initial peak parameters satisfactorily. The peak data observed in the original curves were used as the initial peak parameters. As required, additional separating peaks were considered. The fitting needed more than 10 separating peaks and was carried out in three divided parts of 1100–700, 700–400, and 400–350 cm^{-1}. The original curves were noisy in the region 400–350 cm^{-1}, because of insufficient energy gain of the spectrometer in this region. For this region only one peak at about 370 cm^{-1} was considered. There exists no theoretical justification in any specific functional form for

TABLE II

PEAK POSITIONS OF IR ACTIVE MODES OF MoO_3 (*7, 8*)

Mode	Calc. freq. (cm^{-1})	ν_{TO}-ν_{LO} (cm^{-1})	
B_{3u} δMo–O2′	333	348	352
B_{2u} δMo–O2′	334	353	363
B_{3u} δMo–O1	358	363	390
B_{2u} δMo–O1	380	388	?
B_{2u} νMo–O2	507	441	505
B_{3u} νMo–O2	507	500	525
A_u νMo–O2′	671	(IR inactive)	
B_{1u} νMo–O2′	671	545	851
B_{2u} νMo–O3′[a]	822	814	825
B_{3u} νMo–O3′[a]	822	818	974
B_{2u} νMo–O1	997	962	1010
B_{3u} νMo–O1	999	1002	

[a] O3 and O3′ are equivalent under the discussion by unit cell group analysis.

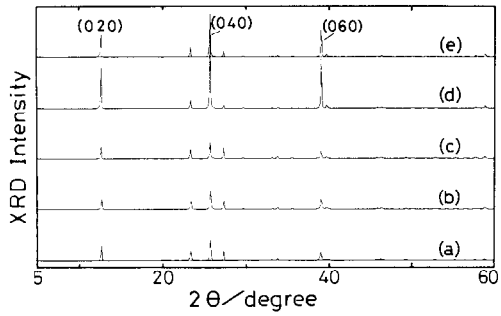

FIG. 3. XRD patterns of the MoO_3 specimens: (a) untreated and after heat treatments (b) at 773 K for 60 min, (c) touching 973 K, (d) at 973 K for 30 min, and (e) at 973 K for 60 min.

IR bands of solids. It is known that a Gaussian form can give satisfactory fitting (*14*). In this work, the best fitting was also achieved using a Gaussian form, although Gaussian and Lorentzian forms were tested.

Results and Discussion

Longitudinal–Transverse Splitting Effects

Figure 3 shows the changes in the XRD pattern of powder MoO_3 with heat treatments. There is no significant change for the specimens after heat treatments at 773 K for 60 min and touching 973 K. By heat treatments at 973 K for 30 and for 60 min, (0 n 0) peaks, n = 2, 4, 6, become intense. This fact indicates some changes in the morphology of crystallites. Integral breadth data of (0 n 0) XRD peaks, n = 2, 4, 6, indicated that there was no change in crystalline size by heating at 773 K, but by heating at 973 K the size became larger than that of the untreated specimen; i.e., sharpening of XRD peaks took place by heating the specimen at 973 K.

Figure 4 shows microphotographs of the specimens. All specimens are composed of crystal slabs (crystallites) with various sizes and various morphologies. The crystallites in untreated specimen have sizes below about 10 μm on their long axes. There were no significant changes in the size of morphology by heating at 773 K for 60 min. By heat treatment touching 973 K the size becomes somewhat larger (about 20 μm) than that of untreated crystallites. There is no significant change in morphology by this treatment. By heating at 973 K for 30–60 min the size becomes much larger and the ratio of sizes between the long and short axes of crystallites becomes apparently larger than that of untreated crystallites (i.e., changes in morphology).

Figure 5 shows changes in IR spectra with the heat treatments. The spectrum exhibits no changes after the treatment at 773 K for 60 min. By heat treatment touching 973 K, the spectrum becomes broader and shows an increase in the intensities of the bands near 500 cm^{-1}. The spectra after the treatments at 973 K for 30–60 min become much broader and apparently contain new peaks or new shoulder peaks. Figure 6 shows the Raman spectrum of the specimen after heat treatment at 973 K for 60 min. This is a typical spectrum of MoO_3. Raman spectra of all other specimens were similar to this and there were no significant changes with the heat treatments.

As described above, the heat treatments give rise to changes in relative intensities among XRD peaks and/or in integral breadths (peak widths), but not in their positions; i.e., these changes are due to the change in morphology and/or size of crystallites, but not in crystal structure. These changes are confirmed by optical microscopy. The changes were followed by the large changes in IR spectra and no change in Raman spectra. This difference between IR and Raman results can be explained by considering longitudinal–transverse splitting effects. As described in the basic background, IR active bands are influenced by the changes in size and morphology of

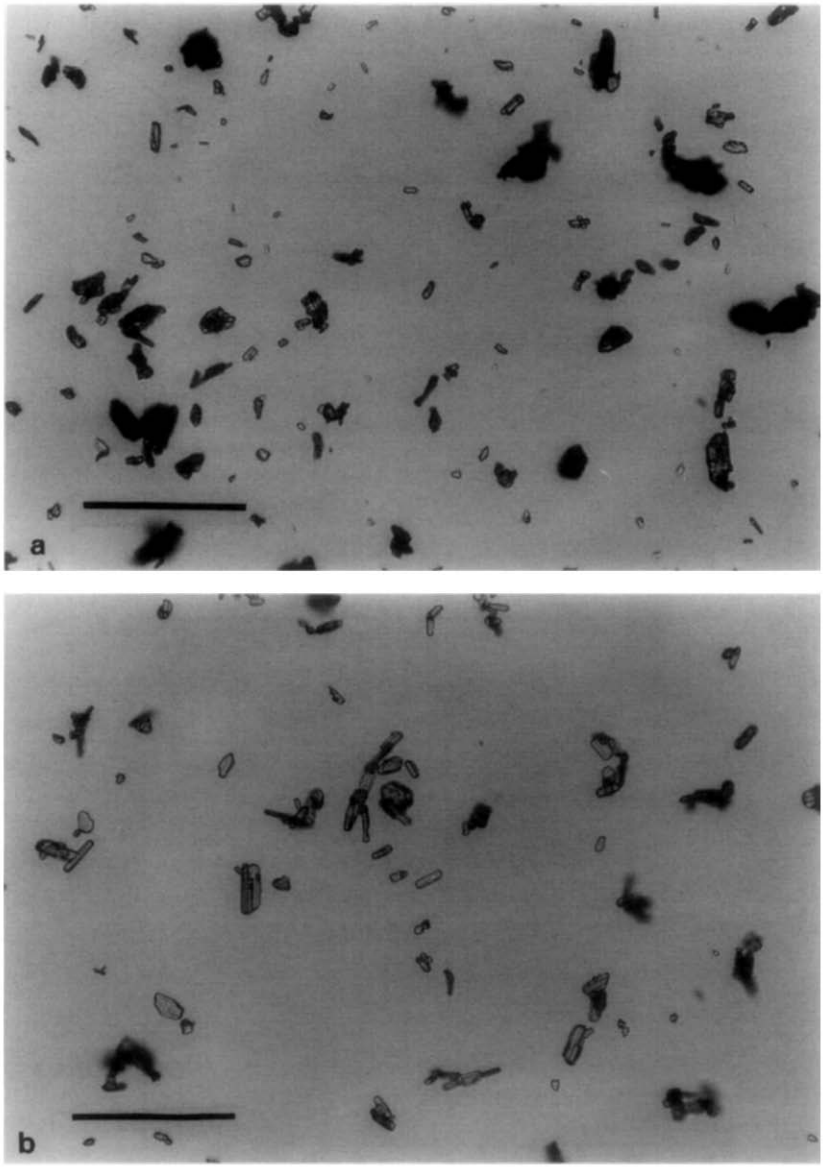

FIG. 4. Optical microphotographs of the specimens: (a) untreated and after heat treatments (b) touching 973 K, (c) at 973 K for 30 min, and (d) at 973 K for 60 min. Scale bar indicates 50 μm.

crystallites owing to longitudinal–transverse splitting effects. For MoO_3 with factor group symmetry D_{2h}, there are no active vibrational modes for both IR and Raman. (The Raman-active modes of MoO_3 are not active for IR absorption. Therefore, $|\partial\mu/\partial Q| = 0$ and $\nu_{LO} = \nu_{TO}$ for these bands.) Thus, only IR spectra were influenced by the changes with heat treatments. The differences of IR band frequencies in a variety of researchers, which are shown in Table I, may be also due to the differences in size and morphology of used MoO_3 specimens.

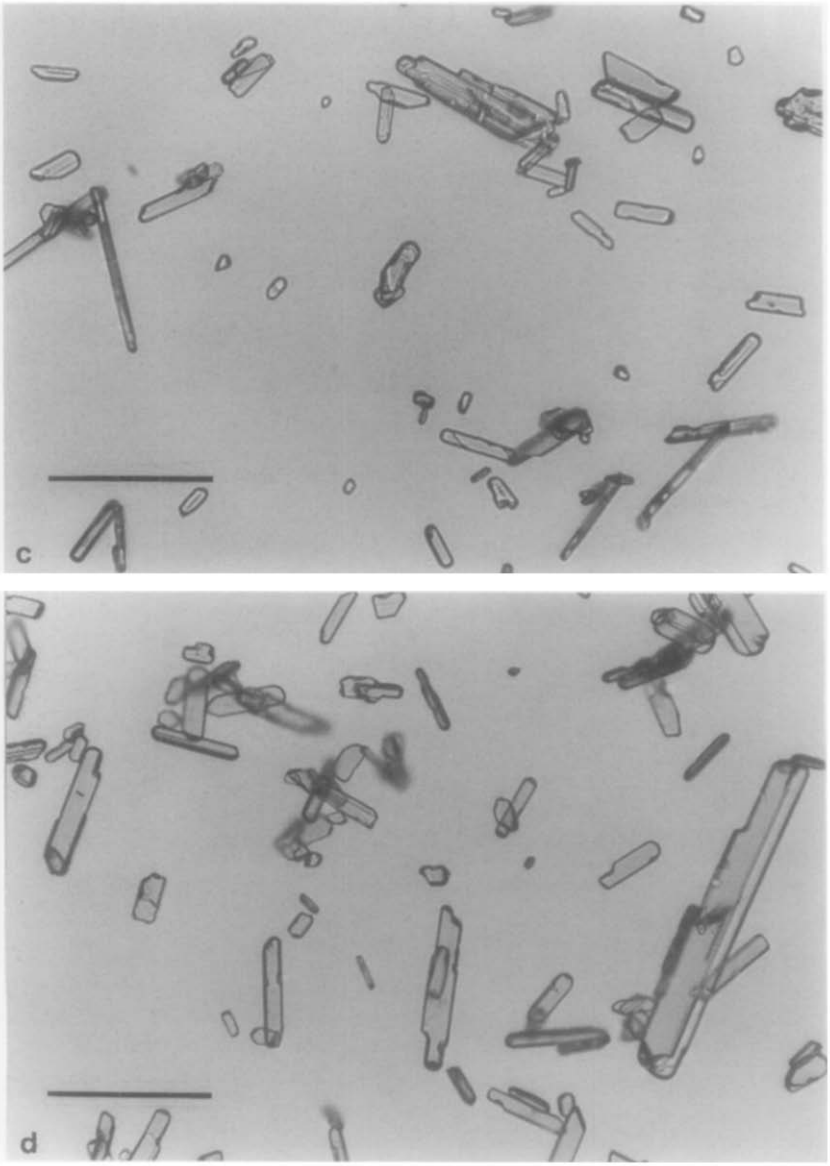

FIG. 4—*Continued*

Assignments of IR Bands

In the measured frequency range, 12 modes are expected by unit cell group analysis. These modes are apparently divided into two groups. The one group is composed of the modes with small $|\partial\mu/\partial Q|$ (i.e., narrow ν_{LO}-ν_{TO} range), while the other is composed of the modes with large $|\partial\mu/\partial Q|$ (i.e., wide ν_{LO}-ν_{TO} range). The ν_{LO}-ν_{TO} ranges are shown in Fig. 5, excluding those of B_{3u} Mo–O2′, B_{2u} Mo–O2′, and B_{2u} Mo–O1 angle deformation modes. As mentioned above, the bands attributed to the modes in the former group are expected to have small intensity and small width, while those attributed to the modes in the latter group are

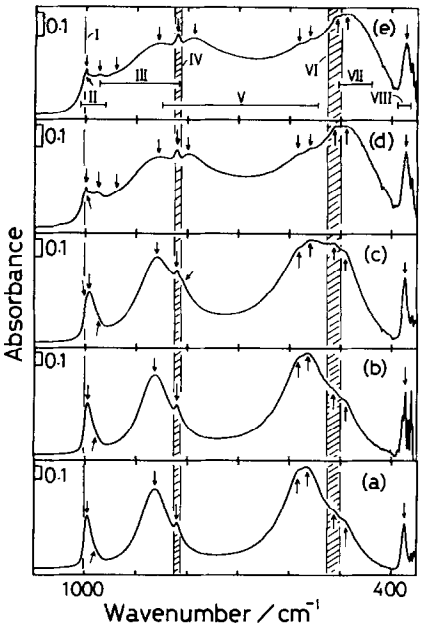

FIG. 5. IR absorption spectra of the MoO_3 specimens: (a) untreated and after heat treatments (b) at 773 K for 60 min, (c) touching 973 K, (d) at 973 K for 30 min, and (e) at 973 K for 60 min. An arrow indicates a peak or a shoulder peak. I–VIII indicate the ν_{LO}-ν_{TO} ranges of B_{3u} Mo–O1, B_{2u} Mo–O1, B_{3u} Mo–O3′, B_{2u} Mo–O3′, B_{1u} Mo–O2′, B_{3u} Mo–O2, and B_{2u} Mo–O2 stretching modes and B_{3u} Mo–O1 angle deformation mode, respectively.

expected to have large intensity and large width. Inspection of Fig. 5 reveals that there are small bands in the ranges of the modes in the former group and large and broad bands in those of the modes in the latter group. (Figure 5(a–c) does not show a small band with narrow width in the range of the B_{3u} Mo–O1 stretching mode apparently, but Fig. 5(d,e) shows such a band. In the ranges of B_{3u} Mo–O2′, B_{2u} Mo–O2′, and B_{2u} Mo–O1 angle deformation modes no definite bands can be observed.) Therefore, the bands in the respective ranges are attributed to the modes based on unit cell group analysis. It is of great advantage to separate the observed spectra into isolated bands, because the separation reveals how the respective bands are influenced by the changes in size and/or morphology of crystallites. Figure 7 shows convolution curves for the specimens untreated and heated at 973 K for 60 min. Before using these convolution results, the author should note a following

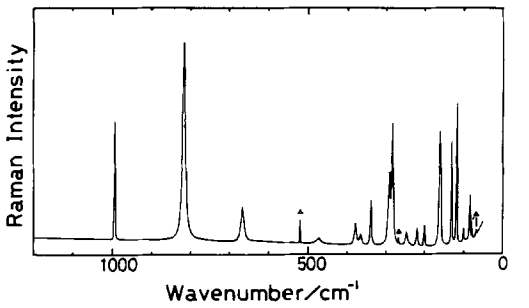

FIG. 6. A Raman spectrum of the MoO_3 specimen heated at 973 K for 60 min. Δ indicates a spontaneous line.

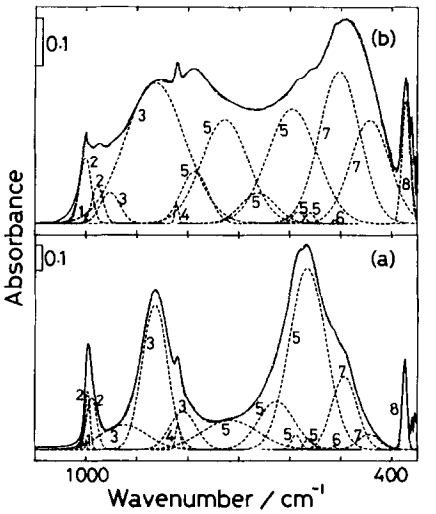

FIG. 7. Curve-resolution results of the IR spectra of the MoO_3 specimens: (a) untreated and (b) heated at 973 K for 60 min. ———: a original curve; — — —: a convolution curve; -----: separating peaks. 1–8 indicate the peaks related to B_{3u} Mo–O1, B_{2u} Mo–O1, B_{3u} Mo–O3′, B_{2u} Mo–O3′, B_{1u} Mo–O2′, B_{3u} Mo–O2, and B_{2u} Mo–O2 stretching modes and B_{3u} Mo–O1 angle deformation mode, respectively.

point: Because the resolution cannot be made on the basis of the information of morphology and size of all the crystallites owing to the complexity of the information (see Fig. 4), the separated peaks, especially those, which are not apparently observed in the original spectra, do not necessarily correspond to physical meaning. As the matter of convenience, the author has resolved the original spectra into the minimum number of separating peaks with Gaussian form using the observed peak data and the separated peaks are substantially related to the modes on unit cell group analysis. (The use of the Gaussian form is appropriate from the shape of the band at about 370 cm^{-1} in Fig. 7(a), which is already isolated in the original spectrum.) The convolution curve for the untreated specimen contains a small peak at 999 cm^{-1}, although the peak is not apparently observed in the original curve. The peak improves the fitting between convolution and original curves. Such a peak is predicted on the basis of the ν_{TO} and ν_{LO} data of Py and Maschke (shown in Table II), and is apparently observed in the original curves for MoO_3 specimens heated at 973 K for 30 min and for 60 min. The author believes that this peak really exists. Judging from intensity, width, and position of the respective separated peaks, they are substantially related to the modes under the unit cell group analysis, as shown in Fig. 7. Figure 8 shows composition of separated peaks related to the respective modes. The separation of the original spectra in Fig. 8 is more proper than that in Fig. 7 to avoid misunderstanding.

Figure 8 indicates that the changes in IR spectra with heat treatments are mainly concerned with B_{2u} Mo–O1, B_{3u} Mo–O3′, B_{1u} Mo–O2′, and B_{2u} Mo–O2 stretching modes and with B_{3u} Mo–O1 angle deformation mode. This fact is reasonable because the modes give rise to a large change of dipole moment, and their peak frequencies and

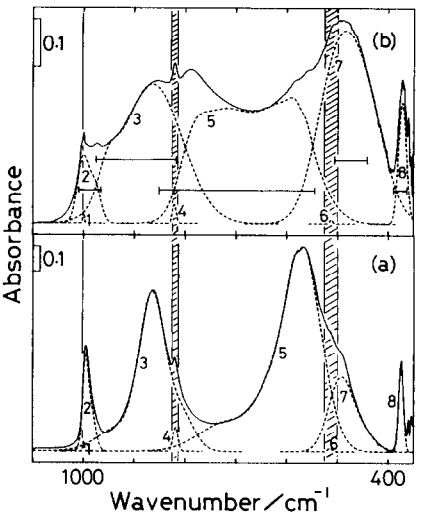

FIG. 8. More proper separation for (a) untreated specimen and (b) specimen heated at 973 K for 60 min. 1–8: see Fig. 7.

band widths are therefore influenced largely by the changes in size and/or morphology of crystallites. (B_{3u} Mo–O1, B_{2u} Mo–O3′, and B_{3u} Mo–O2 stretching modes are scarcely influenced because of their small $|\partial\mu/\partial Q|$.) Then, the bands with wide ν_{LO}-ν_{TO} range are observed as ones with more than two peak maxima. This fact can be understood by considering the coexistence of crystallites with various sizes and various morphologies (Fig. 4). This consideration should be applied to the bands with narrow ν_{LO}-ν_{TO} ranges, but such bands seemingly show one peak maxima owing to the narrow ν_{LO}-ν_{TO} range.

By investigating various specimens depending on the size and morphology of crystallites and by considering longitudinal–transverse splitting effects, detailed interpretations of the IR spectra of powdered MoO_3 were obtained. The changes in IR spectra of MoO_3 result from longitudinal–transverse splitting effects depending on size and/or morphology of crystallites. The procedure used in the present work

gives much advantageous information for assignment of the vibrational bands, although it is necessary to obtain ν_{TO} and ν_{LO} data at the start.

Acknowledgments

The author thanks Professor N. Sotani and Professor T. Takenaka for their useful discussion.

References

1. C. G. Barraclough, J. Lewis, and R. S. Nyholm, *J. Chem. Soc.*, 3552 (1959).
2. C. G. Barraclough and Stals, *Aust. J. Chem.* **19,** 741 (1966).
3. R. Mattes and F. Schröder, *Z. Narturforsch. B: Anorg. Chem., Org. Chem.* **24,** 1095 (1969).
4. I. R. Beattie and T. R. Gilson, *Proc. R. Soc. London, A* **307,** 407 (1968).
5. I. R. Beattie and T. R. Gilson, *J. Chem. Soc. A.*, 2322 (1969).
6. I. R. Beattie, N. Cheetham, Margaret Gardner, and D. E. Rogers, *J. Chem. Soc. A.*, 2240 (1971).
7. M. A. Py, Ph.D. Thesis, Swiss Federal Institute of Technology, Lausanne, Switzerland (1980).
8. M. A. Py and K. Maschke, *Physica B* **105,** 370 (1981).
9. M. Camelot, *Rev. Chim. Miner.* **6,** 853 (1969); R. W. Lovejoy, J. H. Colwell, D. F. Eggers, Jr., and G. D. Halsey, Jr., *J. Chem. Phys.* **36,** 612 (1962).
10. K. G. Ravikumar, S. Rajaraman, and S. Mohan, *Proc. Ind. Natl. Sci. Acad., Part A* **51,** 368 (1985).
11. K. Eda, *J. Solid State Chem.* **83,** 292 (1989). The frequencies calculated using Beattie et al.'s method were reasonably in agreement with the observed IR band frequencies, although the bands also should be influenced with longitudinal-transverse splitting effects. This agreement may result from small longitudinal-transverse splitting effects for H_xMoO_3.
12. P. M. A. Sherwood, "Vibrational Spectroscopy of Solids," Chap. 4, Cambridge Univ. Press, London/New York (1972).
13. L. Kihlborg, *Ark. Kemi.* **21,** 357 (1963).
14. T. Ohno, H. Miyata, F. Hatayama, and N. Sotani, *Bull. Chem. Soc. Jpn.* **60,** 3435 (1987) and references therein.